symmetry

MDPI

Article

Hybrid Functions Approach via Nonlinear Integral Equations with Symmetric and Nonsymmetrical Kernel in Two Dimensions

Sahar M. Abusalim [1], Mohamed A. Abdou [2], Mohamed A. Abdel-Aty [3,*] and Mohamed E. Nasr [1,3]

[1] Department of Mathematics, College of Science and Arts—Gurayat, Jouf University, Sakakah 77454, Saudi Arabia; sabosalem@ju.edu.sa (S.M.A.); menasr@ju.edu.sa (M.E.N.)
[2] Department of Mathematics, Faculty of Education, Alexandria University, Alexandria 21511, Egypt; abdella_777@alexu.edu.eg
[3] Department of Mathematics, Faculty of Science, Benha University, Benha 13518, Egypt
* Correspondence: mohammed.abdallah@fsc.bu.edu.eg

Abstract: The second kind of two-dimensional nonlinear integral equation (NIE) with symmetric and nonsymmetrical kernel is solved in the Banach space $L_2[0,1] \times L_2[0,1]$. Here, the NIE's existence and singular solution are described in this passage. Additionally, we use a numerical strategy that uses hybrid and block-pulse functions to obtain the approximate solution of the NIE in a two-dimensional problem. For this aim, the two-dimensional NIE will be reduced to a system of nonlinear algebraic equations (SNAEs). Then, the SNAEs can be solved numerically. This study focuses on showing the convergence analysis for the numerical approach and generating an estimate of the error. Examples are presented to prove the efficiency of the approach.

Keywords: nonlinear integral equation; symmetric and nonsymmetrical kernel; Banach fixed point theorem; block-pulse function; hybrid functions; Legendre polynomials

MSC: 41A30; 45G10; 46B45; 65R20

check for updates

Citation: Abusalim, S.M.; Abdou, M.A.; Abdel-Aty, M.A.; Nasr, M.E. Hybrid Functions Approach via Nonlinear Integral Equations with Symmetric and Nonsymmetrical Kernel in Two Dimensions. *Symmetry* **2023**, *15*, 1408. https://doi.org/10.3390/sym15071408

Academic Editor: Alexander Zaslavski

Received: 20 June 2023
Revised: 3 July 2023
Accepted: 4 July 2023
Published: 13 July 2023

1. Introduction

Integral equations are used in many disciplines of applied mathematics to explore and solve problems. See [1–6] for more information on the topic of two-dimensional nonlinear integral equations, which have long been of growing interest in many fields, including medicine [7], biology [8], physics [9], geography and fuzzy control [10]. According to the references [11–16], many problems in engineering [17], applied mathematics and mathematical physics [18] can be reduced to two-dimensional nonlinear integral equations with a symmetric and nonsymmetrical kernel. The analytical solutions for these equations are typically difficult. Therefore, it is necessary to use numerical methods or semianalytical methods to obtain the solutions numerically. For example, Bernstein polynomial hybrids with functions of block-pulse form [19,20] and Legendre hybrids with functions of block-pulse form [21,22] have both recently been examined as computational approaches for solving two-dimensional nonlinear integral equations. Alhazmi et al., in [23], used the Lerch polynomial method for solving mixed integral equations in position and time with a strongly symmetric singular kernel. In [24], Azeem et al. conducted research by using the fractional derivative as a treatment for a partial cancer stem cell model. In [25], Attia et al. presented numerical solutions for the fractional differential equations, while in [26], Liaqat et al. presented Shehu transform and the Adomian decomposition technique in a novel algorithm form to establish approximate and exact solutions to quantum mechanics models. Electrical engineering was originally introduced to block-pulse functions by Harmuth; also, other academics have discussed the topic [27].

Recently, hybrid functions have been considered for solving numerous mathematical models, including [28–30]. Using block-pulse functions and Legendre polynomials, Maleknejad and Hashemizadeh described a method for solving mixed-type Hammerstein integral equations [31]. Also, hybrid functions have been applied for solving nonlinear Fredholm–Hammerstein systems. Hesameddini et al., in [32,33], obtained a numerical solution to partial differential equations with nonlocal integration terms. Rafiei et al., in [34] obtained the optimal solution of linear time-delay systems. In [35], Ray and Singh discussed the solution of stochastic Volterra–Fredholm integral equations, numerically using hybrid functions. Hashemzadeh and Maleknejad included the necessary definitions as well as some properties of Legendre polynomials and hybrid block-pulse functions [21].

The focus of this research is how to obtain the numerical solution of nonlinear integral equations with a symmetric and nonsymmetrical kernel in two dimensions. By applying special conditions, we utilize the Banach fixed point theorem to establish the existence and uniqueness of a solution for these equations [36–40]. Our investigation delves into the characteristics of hybrid functions, which are a combination of block-pulse functions and Legendre polynomials. We employ these hybrid functions to solve the integral equations, taking advantage of their useful properties. The approach involves transforming the integral equation into a system of algebraic equations, simplifying and improving the process for finding solutions. Overall, our study provides a novel technique for solving two-dimensional nonlinear integral equations with a symmetric and nonsymmetrical kernel using hybrid functions and demonstrates its effectiveness in obtaining accurate solutions.

The present study is structured into six sections, each focusing on a specific aspect of the numerical approach for solving a two-dimensional nonlinear integral equation with a symmetric and nonsymmetrical kernel. Section 2 delves into the existence and uniqueness of the solution for Equation (1), while Section 3 outlines a method for estimating the solution to this equation. In Section 4, we provide a detailed analysis of the convergence properties of our proposed method. The numerical results obtained from applying this approach are presented in Section 5, followed by concluding remarks in Section 6.

This study aims to present a numerical approach for solving the following two-dimensional nonlinear integral equation with a symmetric and nonsymmetrical kernel approximatively:

$$\begin{aligned}\gamma\psi(x,y) = f(x,y) + \lambda_1 \int_0^1\int_0^1 \Phi(x,\tau;y,v)\mu(\tau,v,\psi(\tau,v))\mathrm{d}v\mathrm{d}\tau \\ + \lambda_2 \int_0^x\int_0^1 G(x,\tau;y,v)\nu(\tau,v,\psi(\tau,v))\mathrm{d}v\mathrm{d}\tau,\end{aligned} \tag{1}$$

where λ_1 and λ_2 are constant scalers having several physical meanings; the function $\psi(x,y)$ is unknown in the Banach spaces $L_2[0,1]\times L_2[0,1]$. The kernels $\Phi(x,\tau;y,v)$ and $G(x,\tau;y,v)$ are continuous in the same space, and the known function $f(x,y)$ is continuous in the space $L_2[0,1]\times L_2[0,1]$. In addition, the constant γ defines the kind of nonlinear integral equations.

2. Existence of a Unique Solution for the Integral Equation with Symmetric and Nonsymmetrical Kernel

The existence of a unique solution of problem (1) is discussed and proved in this section using the Banach fixed point theorem. For this, we write Equation (1) in the form of an integral operator:

$$\overline{V}\psi(x,y) = \frac{1}{\gamma}f(x,y) + V\psi(x,y); \quad \gamma \neq 0, \tag{2}$$

where

$$V\psi(x,y) = \frac{\lambda_1}{\gamma}\int_0^1\int_0^1 \Phi(x,\tau;y,v)\mu(\tau,v,\psi(\tau,v))\mathrm{d}v\mathrm{d}\tau + \frac{\lambda_2}{\gamma}\int_0^x\int_0^1 G(x,\tau;y,v)\nu(\tau,v,\psi(\tau,v))\mathrm{d}v\mathrm{d}\tau. \tag{3}$$

We assume the following conditions:

(i) The kernels $\Phi(x,\tau;y,v)$ and $G(x,\tau;y,v)$ satisfy the following conditions: $\|\Phi(x,\tau;y,v)\| \leq A_1$, $\|G(x,\tau;y,v))\| \leq A_2$, where A_1 and A_2 are two constants, assume $A = \max\{A_1, A_2\}$.

(ii) $\|f(x,y)\| = \left[\int_0^1\int_0^1 |f(x,y)|^2\mathrm{d}x\mathrm{d}y\right]^{\frac{1}{2}} = D,\ D$ is a constant.

(iii) The function $\mu(x,y,\psi(x,y))$ satisfies the following conditions:

$$\|\mu(x,y,\psi(x,y))\| = \left[\int_0^1\int_0^1 |\mu(x,y,\psi(x,y))|^2\mathrm{d}x\mathrm{d}y\right]^{\frac{1}{2}} \leq M_1\|\psi(x,y)\| \tag{4}$$

$$\|\mu(x,y,\psi_1(x,y)) - \mu(x,y,\psi_2(x,y))\| \leq M_2\|\psi_1(x,y) - \psi_2(x,y)\|, \tag{5}$$

where M_1 and M_2 are constants.

(iv) The function $\nu(x,y,\psi(x,y))$ is bounded and satisfies the following:

$$\|\nu(x,y,\psi(x,y))\| = \left[\int_0^1\int_0^1 |\nu(x,y,\psi(x,y))|^2\mathrm{d}x\mathrm{d}y\right]^{\frac{1}{2}} \leq N_1\|\psi(x,y)\| \tag{6}$$

$$\|\nu(x,y,\psi_1(x,y)) - \nu(x,y,\psi_2(x,y))\| \leq N_2\|\psi_1(x,y) - \psi_2(x,y)\|, \tag{7}$$

where, N_1 and N_2 are constants.

Theorem 1. *Assume that the conditions (i)–(iv) are satisfied. Then, Equation (1) has a unique solution $\psi(x,y)$ in the space $L_2[0,1]\times L_2[0,1]$, if the condition*

$$\eta = A\left|\frac{\lambda}{\gamma}\right|[M+N] < 1;\ (\lambda = \max\{\lambda_1,\lambda_2\},\ M = \max\{M_1,M_2\},\ N = \max\{N_1,N_2\}) \tag{8}$$

is true.

To prove the theorem, the following two lemmas must be proven:

Lemma 1. *Under the conditions (i), (ii), (iii-4) and (iv-6), the operator $\overline{V}\psi(x,y)$, defined by Equation (2), maps the space $L_2[0,1]\times L_2[0,1]$ into itself.*

Proof. In light of Formulas (2) and (3), we obtain

$$\|\overline{V}\psi(x,y)\| \leq \frac{1}{|\gamma|}\|f(x,y)\| + \left|\frac{\lambda_1}{\gamma}\right|\left\|\int_0^1\int_0^1 |\Phi(x,\tau;y,v)|\mu(\tau,v,\psi(\tau,v))\mathrm{d}v\mathrm{d}\tau\right\| + \left|\frac{\lambda_2}{\gamma}\right|\left\|\int_0^x\int_0^1 |G(x,\tau;y,v)|\nu(\tau,v,\psi(\tau,v))\mathrm{d}v\mathrm{d}\tau\right\|.$$

From conditions (i) and (ii), we obtain

$$\|\overline{V}\psi(x,y)\| \leq \frac{D}{|\gamma|} + A\left|\frac{\lambda_1}{\gamma}\right|\left\|\int_0^1\int_0^1 |\mu(\tau,v,\psi(\tau,v))\mathrm{d}v\mathrm{d}\tau\right\| + A\left|\frac{\lambda_2}{\gamma}\right|\left\|\int_0^x\int_0^1 \nu(\tau,v,\psi(\tau,v))\mathrm{d}v\mathrm{d}\tau\right\|.$$

Given conditions $(iii\text{-}4)$ and $(iv\text{-}6)$, the above inequality takes on the following form:

$$\|\overline{V}\psi(x,y)\| \le \frac{D}{|\gamma|} + AM\|\psi(x,y)\|\left|\frac{\lambda_1}{\gamma}\right|\left\|\int_0^1\int_0^1 \mathrm{d}v\mathrm{d}\tau\right\| + AN\|\psi(x,y)\|\left|\frac{\lambda_2}{\gamma}\right|\left\|\int_0^x\int_0^1 \mathrm{d}v\mathrm{d}\tau\right\|,$$

where $\max_{0\le x\le 1}|x| = 1$, so that the last inequality becomes

$$\|\overline{V}\psi(x,y)\| \le \frac{D}{|\gamma|} + A\left|\frac{\lambda}{\gamma}\right|[M+N]\|\psi(x,y)\|,$$

since

$$\|\overline{V}\psi(x,y)\| \le \frac{D}{|\gamma|} + \eta\|\psi(x,y)\|; \qquad \eta = A\left|\frac{\lambda}{\gamma}\right|[M+N] < 1. \tag{9}$$

According to this inequality, the operator $\overline{V}$ maps the ball $B_r \subset L_2[0,1]\times L_2[0,1]$ into itself, where

$$r = \frac{D}{|\gamma|(1-\eta)}.$$

□

Lemma 2. *If the conditions (i), (iii-5) and (iv-7) are verified, then the operator $\overline{V}\psi(x,y)$ defined by Equation (2) is continuous in the space $L_2[0,1]\times L_2[0,1]$.*

Proof. Suppose two functions, $\Psi_1(x,y)$ and $\Psi_2(x,y)$, satisfy Equation (2). Then,

$$\overline{V}\psi_1(x,y) - \overline{V}\psi_2(x,y) = \frac{\lambda_1}{\gamma}\int_0^1\int_0^1 \Phi(x,\tau;y,v)[\mu(\tau,v,\psi_1(\tau,v)) - \mu(\tau,v,\psi_2(\tau,v))]\mathrm{d}v\mathrm{d}\tau + \frac{\lambda_2}{\gamma}\int_0^x\int_0^1 G(x,\tau;y,v)[\nu(\tau,v,\psi_1(\tau,v)) - \nu(\tau,v,\psi_2(\tau,v))]\mathrm{d}v\mathrm{d}\tau,$$

applying the properties of the norm, we obtain

$$\|\overline{V}\psi_1(x,y) - \overline{V}\psi_2(x,y)\| \le \left|\frac{\lambda_1}{\gamma}\right|\left\|\int_0^1\int_0^1 |\Phi(x,\tau;y,v)||\mu(\tau,v,\psi_1(\tau,v)) - \mu(\tau,v,\psi_2(\tau,v))|\mathrm{d}v\mathrm{d}\tau\right\| + \left|\frac{\lambda_2}{\gamma}\right|\left\|\int_0^x\int_0^1 |G(x,\tau;y,v)||\nu(\tau,v,\psi_1(\tau,v)) - \nu(\tau,v,\psi_2(\tau,v))|\mathrm{d}v\mathrm{d}\tau\right\|.$$

In view of the conditions (i), $(iii\text{-}5)$ and $(iv\text{-}7)$, the above inequality becomes

$$\|\overline{V}\psi_1(x,y) - \overline{V}\psi_2(x,y)\| \le A\left|\frac{\lambda}{\gamma}\right|[M+N]\|\psi_1(x,y) - \psi_2(x,y)\|,$$

since

$$\|\overline{V}\psi_1(x,y) - \overline{V}\psi_2(x,y)\| \le \eta\|\psi_1(x,y) - \psi_2(x,y)\|.$$

This inequality shows that $\overline{V}$ is a continuous operator in $L_2[0,1]\times L_2[0,1]$. Moreover, $\overline{V}$ is a contraction operator under the condition $\eta < 1$.

The previous two Lemmas 1 and 2 show that the operator $\overline{V}$ defined by (2) is a contraction operator in the space $L_2[0,1]\times L_2[0,1]$. Hence, from the Banach fixed point theorem, $\overline{V}$ has a unique fixed point which is, of course, the unique solution of Equation (1). □

3. Method of Solution for the Main Problem

This section applies the collocation method, two-dimensional hybrid functions and the Gauss quadrature formula to transform the integral Equation (1) into nonlinear systems of equations. The following results are obtained by expanding the function $\Psi(x,y)$ in Equation (1) with respect to two-dimensional hybrid functions:

$$\Psi(x,y) = \sum_{m_1=1}^{\infty}\sum_{n_1=0}^{\infty}\sum_{m_2=1}^{\infty}\sum_{n_2=0}^{\infty} c_{m_1n_1m_2n_2}h_{m_1n_1m_2n_2}(x,y), \tag{10}$$

where the finite series in Equation (10) can be written as

$$\Psi_{S,K}(x,y) = \sum_{m_1=1}^{S}\sum_{n_1=0}^{K-1}\sum_{m_2=1}^{S}\sum_{n_2=0}^{K-1} c_{m_1n_1m_2n_2}h_{m_1n_1m_2n_2}(x,y). \tag{11}$$

where $c_{m_1n_1m_2n_2}$, $m_1, m_2 = 1,2,\ldots,S,\ n_1,n_2 = 0,1,2,\ldots,K-1$, and S, K are the unknown hybrid coefficients.

Substituting Equation (11) into Equation (1) yields

$$\begin{aligned}\gamma\psi_{S,K}(x,y) = f(x,y) &+ \lambda_1 \int_0^1\int_0^1 \Phi(x,\tau;y,v)\mu(\tau,v,\psi_{S,K}(\tau,v))\mathrm{d}v\mathrm{d}\tau \\ &+ \lambda_2 \int_0^x\int_0^1 G(x,\tau;y,v)\nu(\tau,v,\psi_{S,K}(\tau,v))\mathrm{d}v\mathrm{d}\tau.\end{aligned} \tag{12}$$

Now, we discretize Equation (12) at the set of collocation nodes (x_m, y_n) for $m,n = 1,2,\ldots,SK$ as follows:

$$\begin{aligned}\gamma\psi_{S,K}(x_m,y_n) = f(x_m,y_n) &+ \lambda_1 \int_0^1\int_0^1 \Phi(x_m,\tau;y_n,v)\mu(\tau,v,\psi_{S,K}(\tau,v))\mathrm{d}v\mathrm{d}\tau \\ &+ \lambda_2 \int_0^{x_m}\int_0^1 G(x_m,\tau;y_n,v)\nu(\tau,v,\psi_{S,K}(\tau,v))\mathrm{d}v\mathrm{d}\tau,\end{aligned} \tag{13}$$

where

$$x_m = \frac{1}{2}\left(\cos\left(\frac{(2m-1)\pi}{2SK}\right)+1\right),\ m = 1,2,\ldots,SK,$$

and

$$y_n = \frac{1}{2}\left(\cos\left(\frac{(2n-1)\pi}{2SK}\right)+1\right),\ n = 1,2,\ldots,SK,$$

the integral operators in Equation (13) are approximated by using the Gauss–Legendre quadrature formula. For this, we use the following transformations to convert the integrals over $[0,1]$ into the integral over $[-1,1]$,

$$\begin{aligned}\xi &= 2\tau - 1;\ \tau \in [0,1], \\ \varrho &= 2v - 1;\ v \in [0,1].\end{aligned}$$

The integral over $[0, x_m]$ must also be changed into the integral over $[-1,1]$, having the following form

$$\bar{\xi} = \frac{2}{x_m}\tau - 1;\ \tau \in [0, x_m].$$

Then, Equation (13) is converted to

$$\begin{aligned}&\gamma\psi_{S,K}(x_m,y_n) = f(x_m,y_n) \\ &+\frac{\lambda_1}{4}\int_{-1}^1\int_{-1}^1 \Phi(x_m,\frac{1}{2}(\xi+1);y_n,\frac{1}{2}(\varrho+1))\mu(\frac{1}{2}(\xi+1),\frac{1}{2}(\varrho+1),\psi_{S,K}(\frac{1}{2}(\xi+1),\frac{1}{2}(\varrho+1)))\mathrm{d}\varrho\mathrm{d}\xi \\ &+\frac{\lambda_2 x_m}{4}\int_{-1}^1\int_{-1}^1 G(x_m,\frac{x_m}{2}(\bar{\xi}+1);y_n,\frac{1}{2}(\varrho+1)) \\ &\times\nu(\frac{x_m}{2}(\bar{\xi}+1),\frac{1}{2}(\varrho+1),\psi_{S,K}(\frac{x_m}{2}(\bar{\xi}+1),\frac{1}{2}(\varrho+1)))\mathrm{d}\varrho\mathrm{d}\bar{\xi}.\end{aligned}$$

The above equation can be expressed as follows using Gauss–Legendre quadrature:

$$\begin{aligned}
&\gamma\psi_{S,K}(x_m, y_n) = f(x_m, y_n) \\
&\quad + \frac{\lambda_1}{4}\sum_{j=1}^{\ell_1}\sum_{i=1}^{\ell_2} w_j w_i \Phi(x_m, \frac{1}{2}(\xi_i+1); y_n, \frac{1}{2}(\varrho_j+1)) \\
&\quad \times \mu(\frac{1}{2}(\xi_i+1), \frac{1}{2}(\varrho_j+1), \psi_{S,K}(\frac{1}{2}(\xi_i+1), \frac{1}{2}(\varrho_j+1))) \\
&\quad + \frac{\lambda_2 x_m}{4}\sum_{j=1}^{\ell_1}\sum_{i=1}^{\bar{\ell}_2} w_j \bar{w}_i G(x_m, \frac{x_m}{2}(\bar{\xi}_i+1); y_n, \frac{1}{2}(\varrho_j+1)) \\
&\quad \times \nu(\frac{x_m}{2}(\bar{\xi}_i+1), \frac{1}{2}(\varrho_j+1), \psi_{S,K}(\frac{x_m}{2}(\bar{\xi}_i+1), \frac{1}{2}(\varrho_j+1))), \\
&\quad m = 1,2,\ldots,SK, \;\; n = 1,2,\ldots,SK,
\end{aligned} \tag{14}$$

and w_j, w_i and $\bar{w}_i$ are the corresponding weights.

This technique can be used to transform the two-dimensional nonlinear integral problem (1) into a solvable nonlinear system of algebraic equations.

4. Convergence Analysis

The aim of this section is to describe the uniform convergence of the hybrid functions expansion and to determine the maximum absolute truncation error of the function Ψ based on hybrid functions.

Theorem 2. *If $\Psi \in C^4[0,1]$, then the function $\Psi(x,y)$ converges uniformly to the infinite sum of the hybrid functions of $\Psi(x,y)$ described by (10).*

Proof. The hybrid coefficients are defined as

$$\begin{aligned}
c_{m_1n_1m_2n_2} &= \frac{\int_0^1\int_0^1 \Psi(x,y) h_{m_1n_1m_2n_2}(x,y)\mathrm{d}x\mathrm{d}y}{\int_0^1\int_0^1 h^2_{m_1n_1m_2n_2}(x,y)\mathrm{d}x\mathrm{d}y} \\
&= \frac{\int_{\frac{m_2-1}{S}}^{\frac{m_2}{S}}\int_{\frac{m_1-1}{S}}^{\frac{m_1}{S}} \Psi(x,y) L_{n_1}(2Sx-2m_1+1)L_{n_2}(2Sy-2m_2+1)\mathrm{d}x\mathrm{d}y}{\int_{\frac{m_1-1}{S}}^{\frac{m_1}{S}} L^2_{n_1}(2Sx-2m_1+1)\mathrm{d}x \int_{\frac{m_2-1}{S}}^{\frac{m_2}{S}} L^2_{n_2}(2Sy-2m_2+1)\mathrm{d}y}.
\end{aligned}$$

Suppose that $2m_1 - 1 = \hat{m}_1$ and $2Sx - \hat{m}_1 = \Im$. Then,

$$\begin{aligned}
c_{m_1n_1m_2n_2} &= \frac{\int_{\frac{m_2-1}{S}}^{\frac{m_2}{S}}\left(\int_{-1}^1 \Psi(\frac{\hat{m}_1+\Im}{2S}, y)L_{n_1}(\Im)\mathrm{d}\Im\right)L_{n_2}(2Sy-2m_2+1)\mathrm{d}y}{\int_{-1}^1 L^2_{n_1}(\Im)\mathrm{d}\Im\int_{\frac{m_2-1}{S}}^{\frac{m_2}{S}} L^2_{n_2}(2Sy-2m_2+1)\mathrm{d}y} \\
&= \frac{(2n_1+1)}{2}\frac{\int_{\frac{m_2-1}{S}}^{\frac{m_2}{S}}\left(\int_{-1}^1 \Psi(\frac{\hat{m}_1+\Im}{2S}, y)L_{n_1}(\Im)\mathrm{d}\Im\right)L_{n_2}(2Sy-2m_2+1)\mathrm{d}y}{\int_{\frac{m_2-1}{S}}^{\frac{m_2}{S}} L^2_{n_2}(2Sy-2m_2+1)\mathrm{d}y}.
\end{aligned}$$

From the technique of integration by parts with regard to $\Im$ and $(2n+1)L_n(\Im) = L'_{n+1}(\Im) - L'_{n-1}(\Im)$, we obtain

$$c_{m_1n_1m_2n_2} = -\frac{1}{2}\frac{\int_{\frac{m_2-1}{S}}^{\frac{m_2}{S}}\left(\int_{-1}^1 \frac{\partial}{\partial\Im}\Psi(\frac{\hat{m}_1+\Im}{2S}, y)(L_{n_1+1}(\Im)-L_{n_1-1}(\Im))\mathrm{d}\Im\right)L_{n_2}(2Sy-2m_2+1)\mathrm{d}y}{\int_{\frac{m_2-1}{S}}^{\frac{m_2}{S}} L^2_{n_2}(2Sy-2m_2+1)\mathrm{d}y}.$$

Once again, integration by parts of the above relation results

$$c_{m_1n_1m_2n_2} = \frac{1}{2}\frac{\int_{\frac{m_2-1}{S}}^{\frac{m_2}{S}}\left(\int_{-1}^{1}\frac{\partial^2}{\partial\Im^2}\Psi(\frac{\hat{m}_1+\Im}{2S},y)[\frac{-L_{n_1}(\Im)}{2n_1+3}-\frac{L_{n_1}(\Im)-L_{n_1-2}(\Im)}{2n_1-1}]\mathrm{d}\Im\right)L_{n_2}(2Sy-2m_2+1)\mathrm{d}y}{\int_{\frac{m_2-1}{S}}^{\frac{m_2}{S}}L_{n_2}^2(2Sy-2m_2+1)\mathrm{d}y}.$$

Now, we have

$$c_{m_1n_1m_2n_2} = \frac{1}{2(2n_1+3)(2n_1-1)}\frac{\int_{\frac{m_2-1}{S}}^{\frac{m_2}{S}}\left(\int_{-1}^{1}\frac{\partial^2}{\partial\Im^2}\Psi(\frac{\hat{m}_1+\Im}{2S},y)\aleph_{n_1}(\Im)\mathrm{d}\Im\right)L_{n_2}(2Sy-2m_2+1)\mathrm{d}y}{\int_{\frac{m_2-1}{S}}^{\frac{m_2}{S}}L_{n_2}^2(2Sy-2m_2+1)\mathrm{d}y},$$

where

$$\aleph_{n_1}(\Im) = (2n_1-1)L_{n_1+2}(\Im) - (4n_1+2)L_{n_1}(\Im) + (2n_1+3)L_{n_1-2}(\Im).$$

Similarly, changing the variable for y as $2m_2-1=\hat{m}_2$, where $2Sy-\hat{m}_2=\wp$, and integrating by parts with respect to $\wp$, we obtain

$$c_{m_1n_1m_2n_2} = \frac{1}{4(2n_1+3)(2n_1-1)(2n_2+3)(2n_2-1)} \int_{-1}^{1}\int_{-1}^{1}\frac{\partial^4}{\partial\wp^2\partial\Im^2}\Psi(\frac{\hat{m}_1+\Im}{2S},\frac{\hat{m}_2+\wp}{2S})\aleph_{n_1}(\Im)\aleph_{n_2}(\wp)\mathrm{d}\Im\mathrm{d}\wp,$$

where

$$\aleph_{n_2}(\wp) = (2n_2-1)L_{n_2+2}(\wp) - (4n_2+2)L_{n_2}(\wp) + (2n_2+3)L_{n_2-2}(\wp).$$

Using the chain derivatives and $\sigma = \max_{(x,y)\in[0,1]}\left|\frac{\partial^4\Psi(x,y)}{\partial x^2\partial y^2}\right|$, it follows that

$$\begin{aligned} c_{m_1n_1m_2n_2} &\le \frac{\sigma}{64S^4(2n_1+3)(2n_1-1)(2n_2+3)(2n_2-1)}\int_{-1}^{1}\int_{-1}^{1}|\aleph_{n_1}(\Im)||\aleph_{n_2}(\wp)|\mathrm{d}\Im\mathrm{d}\wp, \\ &\le \frac{\sigma}{64m_1^2m_2^2(2n_1+3)(2n_1-1)(2n_2+3)(2n_2-1)}\int_{-1}^{1}\int_{-1}^{1}|\aleph_{n_1}(\Im)||\aleph_{n_2}(\wp)|\mathrm{d}\Im\mathrm{d}\wp. \end{aligned} \tag{15}$$

However,

$$\begin{aligned} \left(\int_{-1}^{1}|\aleph_{n_1}(\Im)|\mathrm{d}\Im\right)^2 &= \left(\int_{-1}^{1}|(2n_1-1)L_{n_1+2}(\Im)-(4n_1+2)L_{n_1}(\Im)+(2n_1+3)L_{n_1-2}(\Im)|\mathrm{d}\Im\right), \\ &\le 2\int_{-1}^{1}|(2n_1-1)^2L_{n_1+2}^2(\Im)+(4n_1+2)^2L_{n_1}^2(\Im)+(2n_1+3)^2L_{n_1-2}^2(\Im)|\mathrm{d}\Im, \end{aligned}$$

from the Legendre orthogonal polynomial property, we obtain

$$\left(\int_{-1}^{1}|\aleph_{n_1}(\Im)|\mathrm{d}\Im\right)^2 \le \frac{24(2n_1+3)^2}{2n_1-3}, \tag{16}$$

thus

$$\int_{-1}^{1}|\aleph_{n_1}(\Im)|\mathrm{d}\Im \le \frac{2\sqrt{6}(2n_1+3)}{\sqrt{2n_1-3}} \tag{17}$$

and

$$\int_{-1}^{1}|\aleph_{n_2}(\wp)|\mathrm{d}\wp \le \frac{2\sqrt{6}(2n_2+3)}{\sqrt{2n_2-3}}. \tag{18}$$

By substituting (17) and (18) into (15), we obtain

$$
\begin{aligned}
c_{m_1n_1m_2n_2} &\leq \frac{24\sigma}{64m_1^2m_2^2(2n_1-1)(2n_2-1)\sqrt{(2n_1-3)}\sqrt{(2n_2-3)}}, \\
&\leq \frac{3\sigma}{8m_1^2m_2^2(2n_1-3)^{\frac{3}{2}}(2n_2-3)^{\frac{3}{2}}}.
\end{aligned} \tag{19}
$$

Therefore, the following series is absolutely convergent:

$$
\begin{aligned}
|\Psi(x,y)| &= \left|\sum_{m_1=1}^{\infty}\sum_{n_1=0}^{\infty}\sum_{m_2=1}^{\infty}\sum_{n_2=0}^{\infty} c_{m_1n_1m_2n_2}h_{m_1n_1m_2n_2}(x,y)\right| \\
&\leq \sum_{m_1=1}^{\infty}\sum_{n_1=0}^{\infty}\sum_{m_2=1}^{\infty}\sum_{n_2=0}^{\infty} |c_{m_1n_1m_2n_2}| \\
&< \infty,
\end{aligned}
$$

and the series (10) converges to the function $\Psi(x,y)$ uniformly. □

Theorem 3. *The maximum absolute truncation error of the series solution (10) to nonlinear integral Equation (1) is*

$$
\|\Psi(x,y)-\Psi_{S,K}(x,y)\| \leq \frac{3\sigma}{8S}\left(\sum_{m_1=S+1}^{\infty}\frac{1}{m_1^4}\sum_{n_1=K}^{\infty}\frac{1}{(2n_1-3)^4}\sum_{m_2=S+1}^{\infty}\frac{1}{m_2^4}\sum_{n_2=K}^{\infty}\frac{1}{(2n_2-3)^4}\right)^{\frac{1}{2}}.
$$

Proof.

$$
\begin{aligned}
&\|\Psi(x,y)-\Psi_{S,K}(x,y)\| \\
&\leq \left(\sum_{m_1=S+1}^{\infty}\sum_{n_1=K}^{\infty}\sum_{m_2=S+1}^{\infty}\sum_{n_2=K}^{\infty} c^2_{m_1n_1m_2n_2}\int_0^1\int_0^1 h^2_{m_1n_1m_2n_2}(x,y)\mathrm{d}x\mathrm{d}y\right)^{\frac{1}{2}}.
\end{aligned}
$$

Using the orthogonality property of hybrid functions and taking relation (19) into consideration, we obtain

$$
\begin{aligned}
\|\Psi(x,y)-\Psi_{S,K}(x,y)\| &\leq \left(\sum_{m_1=S+1}^{\infty}\sum_{n_1=K}^{\infty}\sum_{m_2=S+1}^{\infty}\sum_{n_2=K}^{\infty} c^2_{m_1n_1m_2n_2}\frac{1}{S^2(2n_1+1)(2n_2+1)}\right)^{\frac{1}{2}} \\
&\leq \frac{3\sigma}{8S}\left(\sum_{m_1=S+1}^{\infty}\frac{1}{m_1^4}\sum_{n_1=K}^{\infty}\frac{1}{(2n_1-3)^4}\sum_{m_2=S+1}^{\infty}\frac{1}{m_2^4}\sum_{n_2=K}^{\infty}\frac{1}{(2n_2-3)^4}\right)^{\frac{1}{2}}.
\end{aligned}
$$

□

5. Application and Numerical Results

In order to show the accuracy and efficiency of the proposed method, some numerical examples are given in this section. We introduce the following notation to study the absolute values of this method's errors:

$$
R_{S,K} = |\Psi(x,y)-\Psi_{S,K}(x,y)|,
$$

where $\Psi(x,y)$ and $\Psi_{S,K}(x,y)$ are the exact solution and the approximate solution of the integral equations, respectively.

Example 1. *Consider the following two-dimensional nonlinear integral equation with a symmetric and nonsymmetrical kernel:*

$$16\psi(x,y) = f(x,y) + \int_0^1 \int_0^1 (x\tau + yv)\psi^2(\tau,v)\mathrm{d}v\mathrm{d}\tau + \int_0^x \int_0^1 (x^2\tau^2 + yv)\psi^2(\tau,v)\mathrm{d}v\mathrm{d}\tau, \quad (20)$$

where

$$f(x,y) = \frac{-7}{24} - \frac{28yx}{45} + 16(x^2+y^2) - \frac{x^2y^2}{360}(30y^4 + 72y^5x + 45y^2x^2 + 80y^3x^3 + 30x^4 + 72yx^5).$$

Exact solution is $\psi(x,y) = x^2 + y^2$, using the proposed numerical technique, where $S = 2$ and $K = 2,4,6,8$ in the interval $[0,1)$.

In Table 1, we present the absolute error $|\Psi(x,y) - \Psi_{S,K}(x,y)|$, using the introduced numerical method with $S = 2$ and $K = 2,4,6,8$ in the interval $[0,1)$. Table 2 shows the maximum absolute errors of the given method.

Table 1. Absolute error of solution of Equation (20) by using the present method with $S = 2$ and $K = 2,4,6,8$.

(x_i, y_i)	$S = 2$, $K = 2$	$S = 2$, $K = 4$	$S = 2$, $K = 6$	$S = 2$, $K = 8$
(0, 0)	5.62845×10^{-9}	3.25447×10^{-10}	2.36512×10^{-13}	1.32654×10^{-16}
(0.1, 0.1)	2.51405×10^{-7}	2.36524×10^{-8}	1.36524×10^{-10}	6.32514×10^{-13}
(0.2, 0.2)	5.62103×10^{-6}	2.36985×10^{-7}	5.36214×10^{-9}	8.22551×10^{-12}
(0.3, 0.3)	2.02154×10^{-4}	3.58412×10^{-5}	8.32541×10^{-8}	6.32165×10^{-10}
(0.4, 0.4)	4.58721×10^{-4}	3.65413×10^{-4}	2.21345×10^{-7}	1.32114×10^{-9}
(0.5, 0.5)	7.36212×10^{-4}	2.23651×10^{-4}	3.65221×10^{-7}	2.36985×10^{-8}
(0.6, 0.6)	1.36521×10^{-3}	1.65214×10^{-4}	7.32651×10^{-7}	2.92541×10^{-8}
(0.7, 0.7)	5.26512×10^{-3}	1.36524×10^{-3}	6.32541×10^{-6}	6.32548×10^{-8}
(0.8, 0.8)	5.62514×10^{-2}	4.36210×10^{-3}	8.36251×10^{-6}	7.32614×10^{-8}
(0.9, 0.9)	5.65214×10^{-2}	6.25489×10^{-3}	5.32658×10^{-5}	1.36524×10^{-6}

Moreover, in Figures 1–4, we show a comparison between the exact solution and the approximate solution using the presented numerical technique with different values of $K = 2,4,6,8$ with $S = 2$ in the interval $[0,1)$.

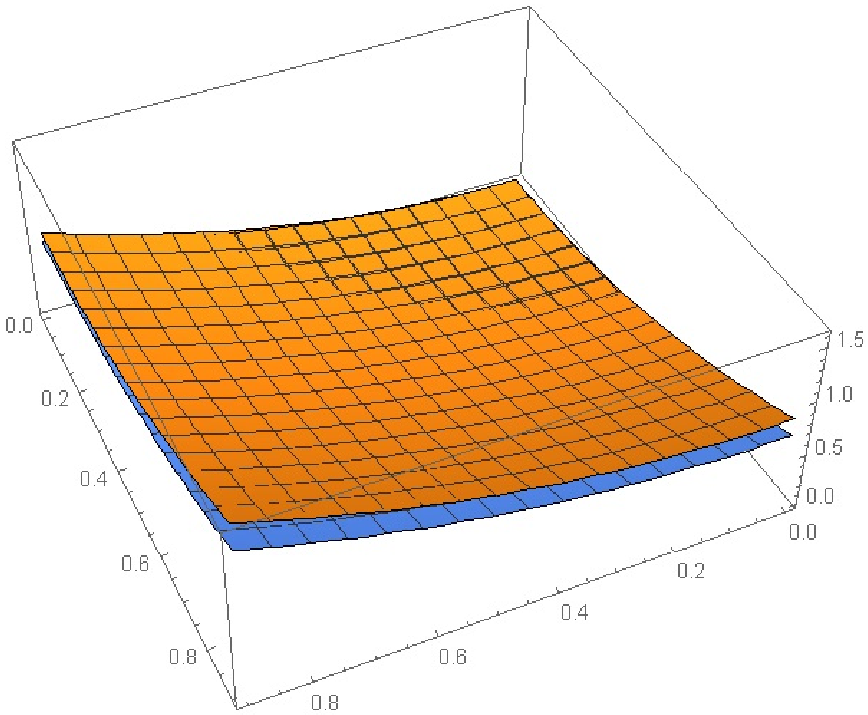

Figure 1. Exact and approximate solution of Equation (20) with $S = 2$ and $K = 2$.

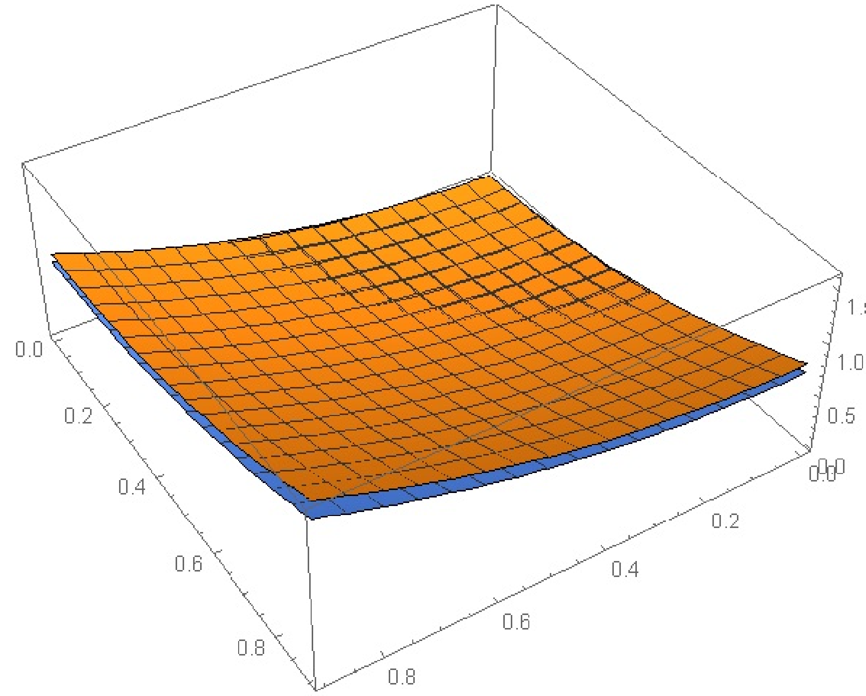

Figure 2. Exact and approximate solution of Equation (20) with $S = 2$ and $K = 4$.

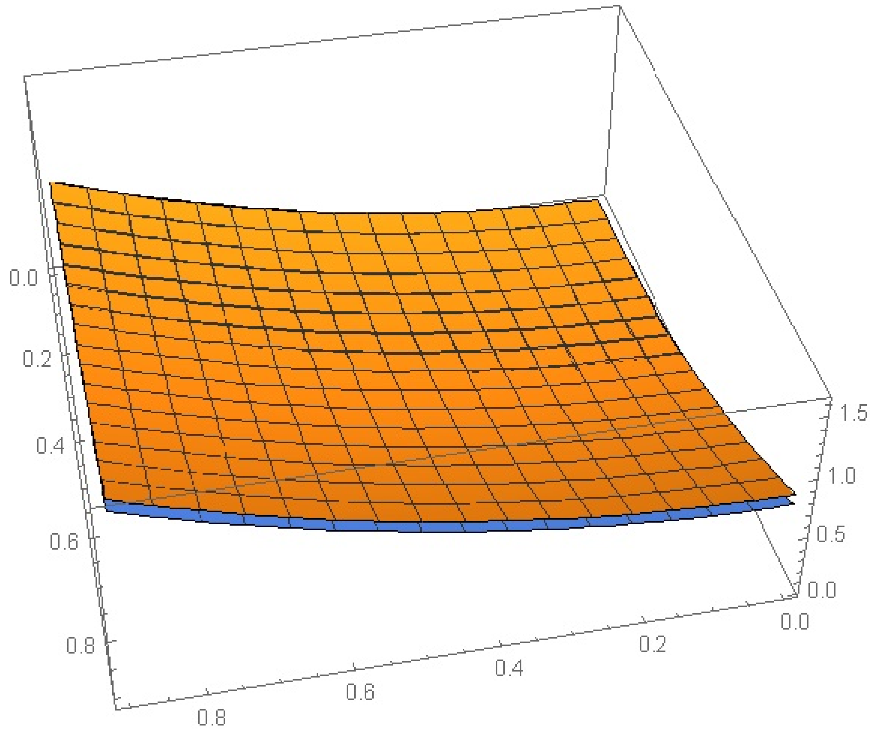

Figure 3. Exact and approximate solution of Equation (20) with $S = 2$ and $K = 6$.

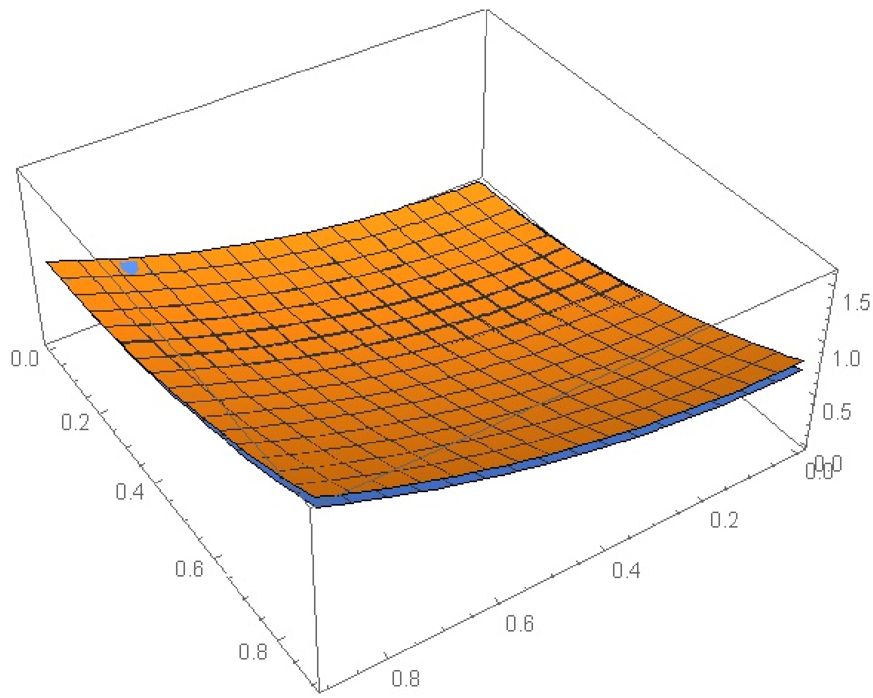

Figure 4. Exact and approximate solution of Equation (20) with $S = 2$ and $K = 8$.

Table 2. The maximum error $R_{max}(x, y)$ for different values of $K = 2, 4, 6, 8$ and $S = 2$ for Equation (20).

	$S = 2$, $K = 2$	$S = 2$, $K = 4$	$S = 2$, $K = 6$	$S = 2$, $K = 8$
R_{max}	6.2103×10^{-2}	6.53210×10^{-3}	5.32658×10^{-5}	1.36524×10^{-6}

Example 2. *Consider the nonlinear integral equation with a symmetric and nonsymmetrical kernel:*

$$\begin{aligned} \psi(x,y) = f(x,y) &+ 0.003\int_0^1\int_0^1 (x\tau^2 + v\cos y)\psi^3(\tau,v)\mathrm{d}v\mathrm{d}\tau \\ &+ 0.003\int_0^x\int_0^1 (x^2\tau + yv)\psi(\tau,v)\mathrm{d}v\mathrm{d}\tau, \end{aligned} \tag{21}$$

where

$$f(x,y) = \frac{1}{12}\Big(27 + 16\cos 1 - 16\cos 2 - 18\cos 3 + 7\cos 4 - 12t^2x(2+\cos 1)\sin(\frac{1}{4})^4$$
$$-12\sin 1 - 36\sin 2 + 6\sin 3 + 6\sin 4) + x\sin y + \frac{1}{2}y^3\Big(-3x^2 + x(2+3x)\cos x - 2\sin x\Big).$$

The exact solution is $\psi(x, y) = x\sin y$, using the presented numerical technique with $S = 2$ and $K = 3, 5, 7, 9$ in the interval $[0, 1)$.

In Table 3, we show the absolute error $|\Psi(x, y) - \Psi_{S,K}(x, y)|$, using the introduced numerical method with $S = 2$ and $K = 3, 5, 7, 9$ in the interval $[0, 1)$. Table 4 shows the maximum absolute errors of the given method.

Table 3. Absolute error of solution of Equation (21) by using the present method with $S = 2$ and $K = 3,5,7,9$.

(x_i, y_i)	$S = 2, K = 3$	$S = 2, K = 5$	$S = 2, K = 7$	$S = 2, K = 9$
(0, 0)	3.20514×10^{-5}	5.32641×10^{-6}	6.32141×10^{-9}	2.36541×10^{-11}
(0.1, 0.1)	3.25481×10^{-4}	9.32541×10^{-5}	5.32187×10^{-7}	3.65874×10^{-8}
(0.2, 0.2)	3.32541×10^{-3}	3.21554×10^{-4}	2.36414×10^{-6}	7.36584×10^{-8}
(0.3, 0.3)	4.32641×10^{-3}	5.32654×10^{-4}	5.32684×10^{-6}	3.36241×10^{-7}
(0.4, 0.4)	5.36854×10^{-3}	6.36524×10^{-4}	8.32546×10^{-6}	6.32584×10^{-7}
(0.5, 0.5)	6.93154×10^{-3}	$7.1.365 \times 10^{-4}$	6.32541×10^{-5}	8.65241×10^{-7}
(0.6, 0.6)	1.32511×10^{-2}	3.21547×10^{-3}	9.99215×10^{-5}	4.32516×10^{-6}
(0.7, 0.7)	4.32658×10^{-2}	4.36561×10^{-3}	1.32154×10^{-4}	8.69854×10^{-6}
(0.8, 0.8)	5.32666×10^{-2}	5.76524×10^{-3}	2.34541×10^{-4}	4.36215×10^{-5}
(0.9, 0.9)	6.32541×10^{-2}	7.96525×10^{-3}	3.25456×10^{-4}	1.05214×10^{-4}

Table 4. The maximum error $R_{max}(x, y)$ for different values of $K = 3,5,7,9$ and $S = 2$ for Equation (21).

	$S = 2, K = 3$	$S = 2, K = 5$	$S = 2, K = 7$	$S = 2, K = 9$
R_{max}	6.32541×10^{-2}	7.96525×10^{-3}	3.25456×10^{-4}	1.05214×10^{-4}

Furthermore, in Figures 5–8, we present a comparison between the exact solution and the approximate solution using the introduced numerical method with different values of $K = 3,5,7,9$ *with* $S = 2$ *in the interval* $[0, 1)$.

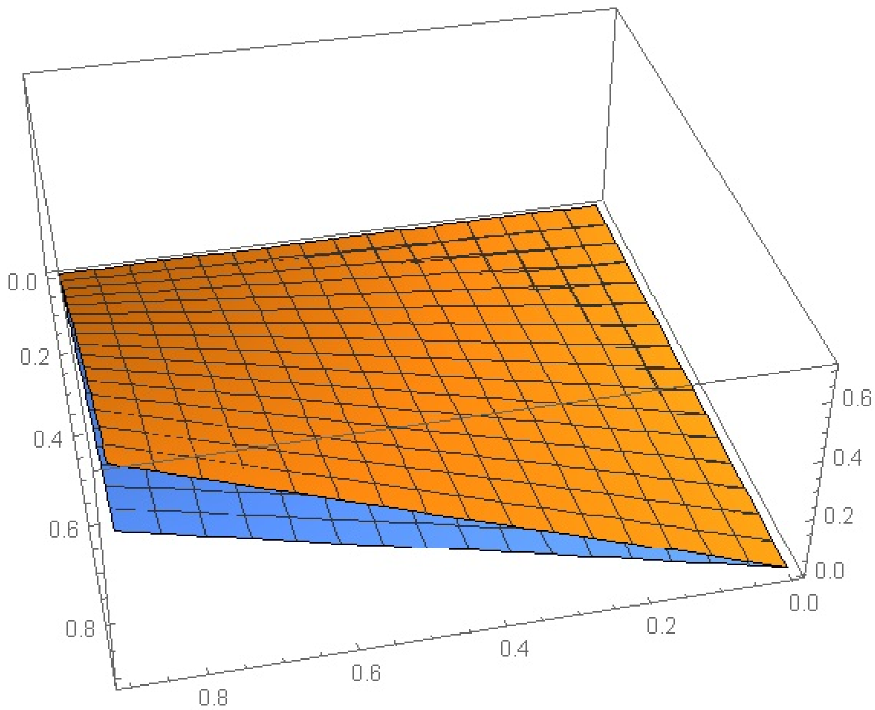

Figure 5. Exact and approximate solution of Equation (21) with $S = 2$ and $K = 3$.

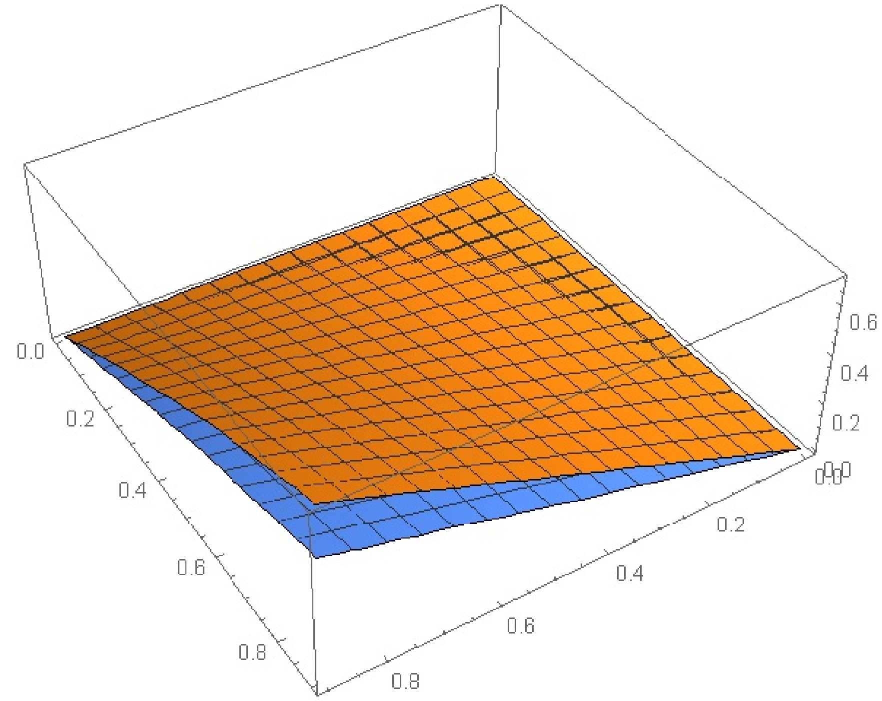

Figure 6. Exact and approximate solution of Equation (21) with $S = 2$ and $K = 5$.

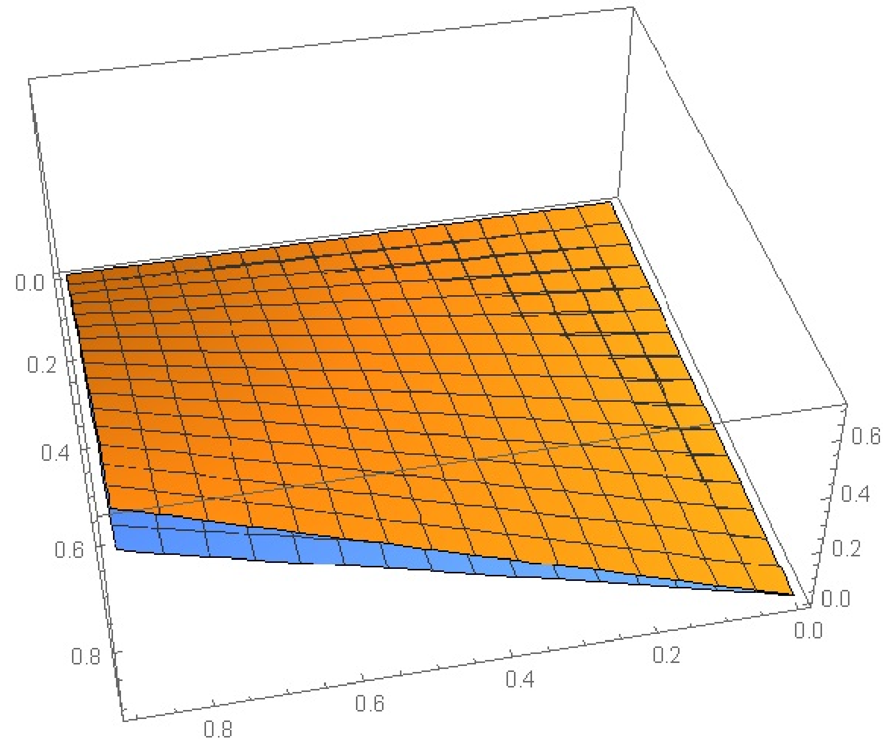

Figure 7. Exact and approximate solution of Equation (21) with $S = 2$ and $K = 7$.

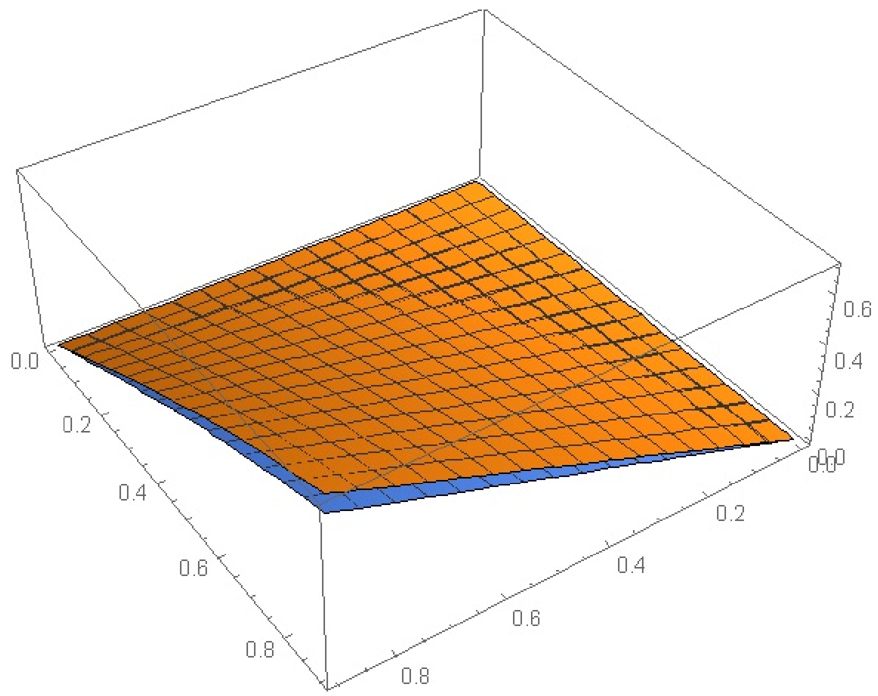

Figure 8. Exact and approximate solution of Equation (21) with $S = 2$ and $K = 9$.

Example 3. *Consider the following two-dimensional nonlinear integral equation with a symmetric and nonsymmetrical kernel:*

$$7\psi(x,y) = f(x,y) + 0.01\int_0^1\int_0^1 (x-y)^2\psi(\tau,v)\mathrm{d}v\mathrm{d}\tau + 0.01\int_0^x\int_0^1(\tau+v)\psi^2(\tau,v)\mathrm{d}v\mathrm{d}\tau, \quad (22)$$

where

$$f(x,y) = 7e^t x - 0.00859141(t-x)^2 - 0.000416667x^3(2-3x+e^{2t}(-2+4t+3x)).$$

The exact solution is $\psi(x,y) = xe^y$, using the proposed numerical technique, where $S = 3$ and $K = 2,3,6,7$ in the interval $[0,1)$.

In Table 5, we present the absolute error $|\Psi(x,y) - \Psi_{S,K}(x,y)|$, using the introduced numerical method with $S = 3$ and $K = 2,3,6,7$ in the interval $[0,1)$. Table 6 shows the maximum absolute errors of the given method.

Table 5. Absolute error of solution of Equation (22) by using the present method with $S = 3$ and $K = 2,3,6,7$

(x_i, y_i)	$S = 3$, $K = 2$	$S = 3$, $K = 3$	$S = 3$, $K = 6$	$S = 3$, $K = 7$
(0, 0)	9.32484×10^{-10}	8.32544×10^{-11}	5.21432×10^{-14}	1.23698×10^{-16}
(0.1, 0.1)	7.62514×10^{-9}	3.52147×10^{-9}	2.81647×10^{-11}	5.21478×10^{-15}
(0.2, 0.2)	5.03698×10^{-7}	3.62149×10^{-8}	3.89759×10^{-10}	2.98547×10^{-13}
(0.3, 0.3)	1.20584×10^{-5}	5.20147×10^{-6}	5.07896×10^{-10}	4.69857×10^{-11}
(0.4, 0.4)	2.96521×10^{-5}	5.36987×10^{-5}	4.36985×10^{-8}	3.21458×10^{-10}
(0.5, 0.5)	4.36514×10^{-5}	5.58741×10^{-5}	5.20142×10^{-8}	3.69521×10^{-9}
(0.6, 0.6)	4.96587×10^{-5}	6.36925×10^{-5}	1.25847×10^{-7}	4.25871×10^{-9}
(0.7, 0.7)	1.32548×10^{-3}	2.01321×10^{-4}	6.87452×10^{-7}	3.02587×10^{-8}
(0.8, 0.8)	3.02584×10^{-3}	3.47585×10^{-4}	1.01024×10^{-6}	4.08754×10^{-8}
(0.9, 0.9)	5.01478×10^{-3}	1.75214×10^{-3}	4.36954×10^{-6}	5.31231×10^{-8}

Moreover, in Figures 9–12, we show a comparison between the exact solution and the approximate solution using the presented numerical technique with different values of $K = 2, 3, 6, 7$ *with* $S = 3$ *in the interval* $[0, 1)$.

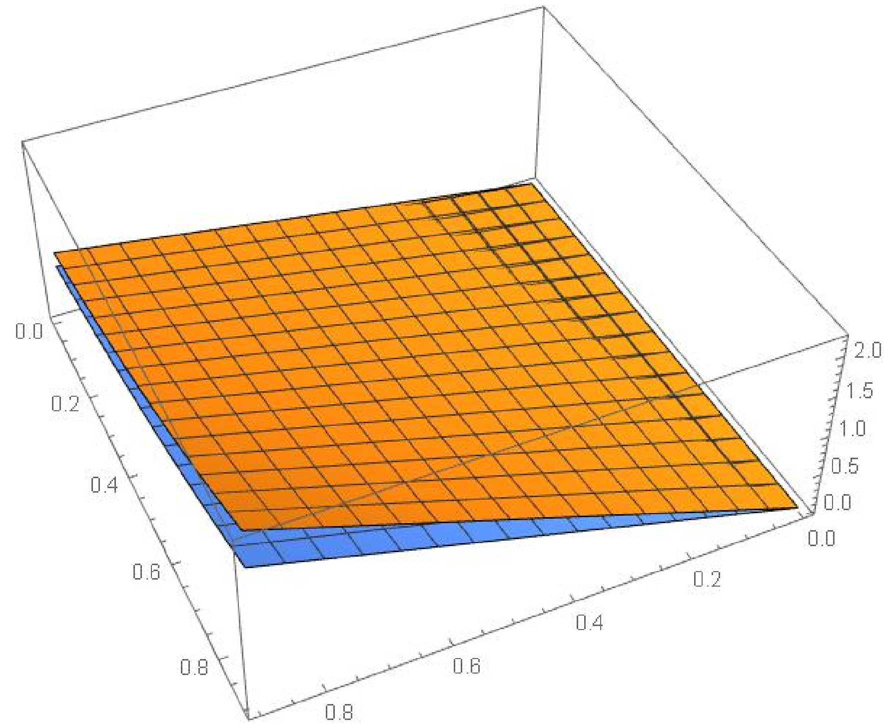

Figure 9. Exact and approximate solution of Equation (22) with $S = 3$ and $K = 2$.

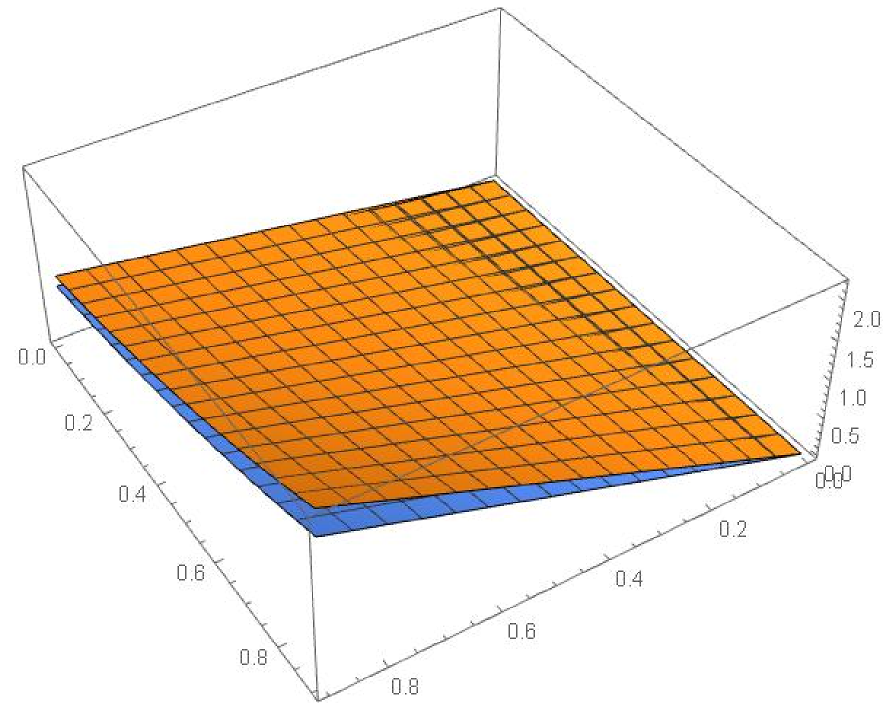

Figure 10. Exact and approximate solution of Equation (22) with $S = 3$ and $K = 3$.

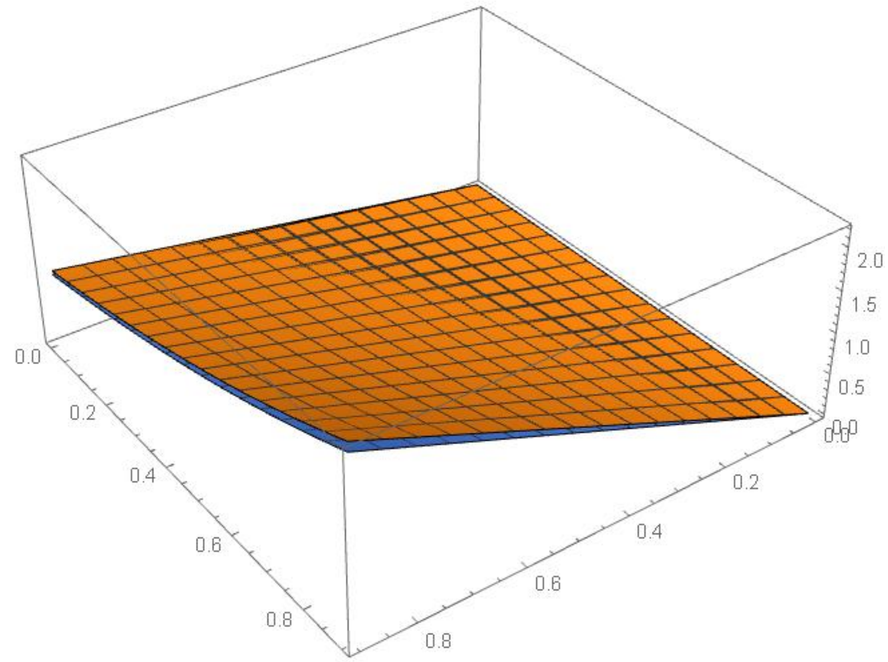

Figure 11. Exact and approximate solution of Equation (22) with $S = 3$ and $K = 6$.

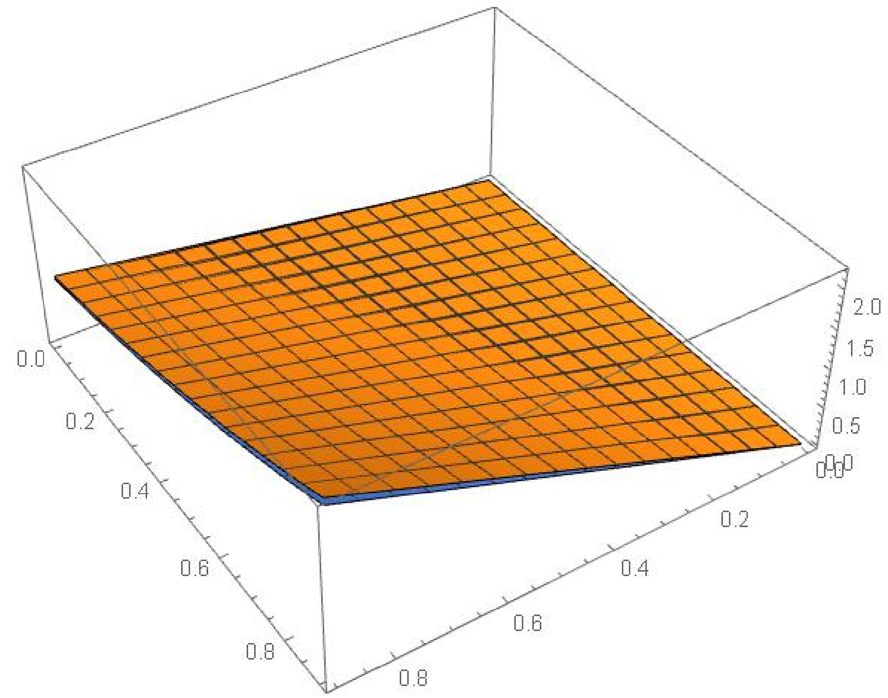

Figure 12. Exact and approximate solution of Equation (22) with $S = 3$ and $K = 7$.

Table 6. The maximum error $R_{max}(x, y)$ for different values of $K = 2, 3, 6, 7$ and $S = 3$ for Equation (22).

	$S = 3$, $K = 2$	$S = 3$, $K = 3$	$S = 3$, $K = 6$	$S = 3$, $K = 7$
R_{max}	5.01478×10^{-3}	1.75214×10^{-3}	4.36954×10^{-6}	5.31231×10^{-8}

6. Conclusions and Remarks

The following can be deduced from the above analysis and discussion:

1. Under some conditions, Equation (1) has a unique solution $\Psi(x, y)$ in the space $L_2[0, 1] \times L_2[0, 1]$.

2. After applying the proposed method, a two-dimensional integral equation with a symmetric and nonsymmetrical kernel of the second kind tends to result in an algebraic system of nonlinear equations.
3. A nonlinear system of algebraic equations has a solution.
4. Three illustrative examples are provided to evaluate and validate the effectiveness and dependability of the proposed method. Tables and Figures are used to show the numerical results. For example, Figures 1, 5 and 9 contained the numerical solution of Examples 1, 2 and 3, respectively, for different values of x, y and K. Figures 1–12 formed the absolute errors of each example with different values of x and y.
5. In Example 1, absolute errors in four cases of K are presented in Table 1 and Figures 1–4. The error increases through x and y. When we take the Max. value error in Figure 1, it is (6.2103×10^{-2}) at $S = 2$, $K = 2$. Also, the Min. error value in Figure 4 is (1.36524×10^{-6}) at $S = 2$, $K = 8$ (see Table 2).
6. In Example 2, from Table 4 at $S = 2$, $K = 3$, the error is as high as possible at point $x = y = 0.9$, and its value is (6.32541×10^{-2}). Likewise, the error begins to decrease, and when the value of $x = y = 0$, its value is (1.05214×10^{-4}).
7. In Example 3, the error decreases as S and K increase, where the maximum value of the error at $x = y = 0.9$ for $S = 3$, $K = 2$ is (5.01478×10^{-3}), while for $S = 3$, $K = 7$, the minimum value of the error is (5.31231×10^{-8}).
8. In general, the error obtained by the proposed method decreases when the number of (K) increases.

7. Future Work

We will consider the following two-dimensional nonlinear integral equation with phase-lag term:

$$\gamma\psi(x+\delta x, y+\delta y) = f(x+\delta x, y+\delta y) + \lambda_1 \int_0^1 \int_0^1 \Phi(x+\delta x, \tau; y+\delta y, v)\mu(\tau, v, \psi(\tau, v))\mathrm{d}v\mathrm{d}\tau$$
$$+ \lambda_2 \int_0^{x+\delta x} \int_0^1 G(x+\delta x, \tau; y+\delta y, v)\nu(\tau, v, \psi(\tau, v))\mathrm{d}v\mathrm{d}\tau.$$

Author Contributions: Conceptualization, M.A.A.; methodology, M.A.A. and M.A.A.-A.; software, M.E.N.; validation, M.A.A.-A.; formal analysis, M.E.N.; resources, M.A.A.-A.; data curation, S.M.A.; writing—original draft, S.M.A., M.A.A., M.A.A.-A. and M.E.N.; writing—review and editing, S.M.A., M.A A., M.A.A.-A. and M.E.N.; supervision, M.A.A.; funding acquisition, S.M.A. All authors have read and agreed to the published version of the manuscript.

Funding: This research received no external funding.

Data Availability Statement: No instructional records have been created or comfortable with the ongoing assessment data in this original copy.

Acknowledgments: The authors would like to thank the reviewers of the journal Mathematics for their valuable comments and advice on the first version of this article.

Conflicts of Interest: The authors declare no conflict of interest.

References

1. Abdou, M.A.; Soliman, A.A.; Abdel-Aty, M.A. On a discussion of Volterra—Fredholm integral equation with discontinuous kernel. *J. Egypt. Math. Soc.* **2020**, *28*, 11. [CrossRef]
2. Bakhshayesh, S.J. Discontinuous Galerkin approximations for Volterra integral equations of the first kind with convolution kernel. *Indian J. Sci. Technol.* **2015**, *8*, 33. [CrossRef]
3. Brezinski, C.; Redivo-Zalglia, M. Extrapolation methods for the numerical solution of nonlinear Fredholm integral equations. *J. Integral Equat. Appl.* **2019**, *31*, 29–57. [CrossRef]
4. Nasr, M.E.; Abdel-Aty, M.A. Analytical discussion for the mixed integral equations. *J. Fixed Point Theory Appl.* **2018**, *20*, 115. [CrossRef]
5. Nasr, M.E.; Abdel-Aty, M.A. A new techniques applied to Volterra–Fredholm integral equations with discontinuous kernel. *J. Comput. Anal. Appl.* **2021**, *29*, 11–24.

6. Mirzaee, F. Numerical solution of system of linear integral equations via improvement of block-pulse functions. *J. Math. Model* **2016**, *4*, 133–159.
7. Abdou, M.A.; Nasr, M.E.; Abdel-Aty, M.A. A study of normality and continuity for mixed integral equations. *J. Fixed Point Theory Appl.* **2018**, *20*, 5. [CrossRef]
8. Hannabou, M.; Bouaouid, M.; Hilal, K. Existence and uniqueness of solutions for a fractional hybrid system with nonseparated integral boundary hybrid conditions. *J. Funct. Spaces* **2022**, *2022*, 3271626. [CrossRef]
9. Golberg, M.A.; Chen, C.S. *Discrete Projection Methods for Integral Equation*; Computational Mechanics Publications: Southampton, UK; Boston, MA, USA, 1997.
10. Hassan, T.S.; Odinaev,I.; Shah, R.; Weera, W. Dynamical analysis of fractional integro-differential equations. *Mathematics* **2022**, *10*, 2071. [CrossRef]
11. Agarwal, R.P.; Alghamdi, A.M.; Gala, S.; Ragusa, M.A. On the regularity criterion on one velocity component for the micropolar fluid equations. *Math. Model. Anal.* **2023**, *28*, 271–284. [CrossRef]
12. Elzaki, T.M.; Alamri, A.S. Note on new homotopy perturbation method for solving nonlinear integral equations. *J. Math. Comput. Sci.* **2016**, *6*, 149–155.
13. Hafez, R.M.; Youssri, Y.H. Spectral Legendre-Chebyshev treatment of 2D linear and nonlinear mixed Volterra-Fredholm integral equation. *Math. Sci. Lett.* **2020**, *9*, 37–47.
14. Gouyandeh, Z.; Allahviranloo, T.; Armand, A. Numerical Solution of Nonlinear Volterra-Fredholm-Hammerstein Integral Equations via Tau-Collocation Method with Convergence Analysis. *J. Comput. Appl. Math* **2016**, *308*, 435–446. [CrossRef]
15. Katani, R. Numerical solution of the Fredholm integral equations with a quadrature method. *SeMA J.* **2019**, *76*, 449–452. [CrossRef]
16. Wang, K.; Wang, Q. Taylor polynomial method and error estimation for a kind of mixed Volterra-Fredholm integral equations. *Appl. Math. Comput.* **2014**, *229*, 53–59. [CrossRef]
17. Chen, Z.; Jiang, W. An Efficient Algorithm for Solving Nonlinear Volterra-Fredholm Integral Equations. *Appl. Math. Comput.* **2015**, *259*, 614–619. [CrossRef]
18. Al-Bugami, A.M. Numerical treating of mixed Integral equation two-dimensional in surface cracks in finite layers of materials. *Adv. Math. Phys.* **2022**, *25*, 3398175. [CrossRef]
19. Alipour, M.; Baleanu, D.; Babaei, F. Hybrid Bernstein block-pulse functions method for second kind integral equations with convergence analysis. *Abstr. Appl. Anal.* **2014**, *2014*, 623763. [CrossRef]
20. Masouri, Z. Numerical expansion-iterative method for solving second kind Volterra and Fredholm integral equations using block-pulse functions. *Adv. Comput. Tech. Electromagn* **2021**, *20*, 7–17. [CrossRef]
21. Hashemzadeh, E.; Maleknejad, K.; Basirat, B. Hybrid functions approach for the nonlinear Volterra–Fredholm integral equations. *Proc. Comput. Sci* **2011**, *3*, 1189–1194. [CrossRef]
22. Marzban, H.R.; Tabrizidooz, H.R.; Razzaghi, M. A composite collection method for the nonlinear mixed Volterra–Fredholm–Hammerstein integral equation. *Commun. Nonlinear Sci. Numer.* **2011**, *16*, 1186–1194. [CrossRef]
23. Alhazmi, S.E.; Mahdy, A.M.; Abdou, M.A.; Mohamed, D.S. Computational Techniques for Solving Mixed (1+1) Dimensional Integral Equations with Strongly Symmetric Singular Kernel. *Symmetry* **2023**, *15*, 1284. [CrossRef]
24. Azeem, M.; Farman, M.; Akgl, A.; Sen, M.D.L. Fractional order operator for symmetric analysis of cancer model on stem cells with chemotherapy. *Symmetry* **2023**, *15*, 533. [CrossRef]
25. Attia, N.; Akgl, A.; Alqahtani, R.T. Extension of the reproducing kernel Hilbert space method's application range to include some important fractional differential equations. *Symmetry* **2023**, *15*, 532. [CrossRef]
26. Liaqat, M.I.; Akgul, A.; Sen, M.D.L.; Bayram, M. Approximate and exact solutions in the sense of conformable derivatives of quantum mechanics models using a novel algorithm. *Symmetry* **2023**, *15*, 744. [CrossRef]
27. Datta, K.B.; Mohan, B.M. *Orthogonal Function in Systems and Control*; World Scientific: Singapore, 1995; Volume 9
28. Mashayekhi, S.; Razzaghi, M. Numerical solution of distributed order fractional differential equations by hybrid functions. *J. Comput. Phys.* **2016**, *315*, 169–181. [CrossRef]
29. Mirzaee, F.; Alipour, S.; Samadyar, N. Numerical solution based on hybrid of Block-pulse and parabolic functions for solving a system of nonlinear stochastic Ito-Volterra integral equations of fractional order. *J. Comput. Appl. Math.* **2019**, *349*, 157–171. [CrossRef]
30. Mohammadi, F.; Moradi, L.; Baleanu, D.; Jajarmi, A. A hybrid functions numerical scheme for fractional optimal control problems: Application to non analytic dynamic systems. *J. Vib. Control* **2017**, *24*, 5030–5043. [CrossRef]
31. Maleknejad, K.; Hashemizadeh, E. Numerical solution of the dynamic model of a chemical reactor by hybrid functions. *Procedia Comput. Sci.* **2011**, *3*, 908–912. [CrossRef]
32. Hesameddini, E.; Riahi, M. Hybrid Legendre Block-pulse functions method for solving partial differential equations with non-local integral boundary conditions. *J. Inf. Optim. Sci.* **2019**, *40*, 1391–1403. [CrossRef]
33. Sahu, P.K.; Saha Ray, S. Hybrid Legendre Block-pulse functions for the numerical solutions of system of nonlinear Fredholm-Hammerstein integral equations. *Appl. Math. Comput.* **2015**, *270*, 871–878. [CrossRef]
34. Rafiei, Z.; Kafash, B.; Karbasi, S.M. State-control parameterization method based on using hybrid functions of Block-pulse and Legendre polynomials for optimal control of linear time delay systems. *Appl. Math. Model* **2017**, *45*, 1008–1019. [CrossRef]
35. Saha Ray, S.; Singh, S. Numerical solution of stochastic Volterra-Fredholm integral equations by hybrid Legendre Block-pulse functions. *Int. J. Nonlinear Sci. Numer.* **2018**, *19*, 289–297. [CrossRef]

36. Ali, F.; Ali, J.; Rodríguez-López, R. Approximation of fixed points and the solution of a nonlinear integral equation. *Nonlinear Funct. Anal. Appl.* **2021**, *26*, 869–885.
37. Bousselse, M.; Kim, D.; Kim, J.K. solvability and asymptotic Behavior of solutions for some nonlinear integral. *Nonlinear Funct. Anal. Appl.* **2023**, *28*, 57–79.
38. El-Deeb, S.M.; Murugusundaramoorthy, G.A. Alburaikan, Bi-Univalent Functions Connected with the Mittag-Leffler-Type Borel Distribution Based Upon the Legendre Polynomials. *Nonlinear Funct. Anal. Appl.* **2022**, *27*, 331–347.
39. Kreyszig, E. *Introductory Functional Analysis with Applications*; John Wiley and Sons, Inc.: New York, NY, USA, 1989.
40. Okeke, G.A.; Kim, J.K. fixed point theorems in complex valued banach spaces with applications to a nonlinear integral equation. *Nonlinear Funct. Anal. Appl.* **2020**, *25*, 411–436. [CrossRef]